

Retrieval of biophysical parameters using directional spectral mixture analysis

F. J. García-Haro, F. Camacho-de Coca and J. Meliá

Department of Thermodynamics, University of Valencia.

C/Dr. Moliner, 50. 46100 Burjassot. Valencia, Spain.

J.Garcia.Haro@uv.es

ABSTRACT

In this study, we propose a modeling scheme to assess angular variation in discontinuous canopies, relating these variations with the main optical and structural parameters. The reflectance of an individual pixel is assumed to consist of an area weighted linear combination of the soil and vegetation radiances. Canopy geometrical effects are considered in the first order scattering. Hot spot kernels are used to model the joint probability of viewed and sunlit components. The model makes a simple treatment of the multiple scattering effect using an approximate analytical solution to the radiative transfer problem. The model formalism and the volume scattering formulation is similar to the GHOST model (Lacaze and Roujean, 2001). However, the between-crown gap probability is formulated in terms of the FVC and a geometric variable (η) associated with the shape of plants. The invertibility of the model to retrieve FVC and LAI was tested using airborne POLDER measurements corresponding to cropland. Although the model is less suited for homogeneous canopies, it has provided reasonable results, similar to accurate BRDF models of homogeneous canopies like NADIM (Gobron et al., 1997).

1 INTRODUCTION

Within the frame of the LSA SAF Project (Satellite Application Facility on Land surface analysis), we are aimed to develop robust and operational algorithms for retrieving biophysical parameters from the future Meteosat Second Generation (MSG) and European Polar System (EPS) satellites. The synergistic use of SEVIRI/MSG and AVHRR-3/EPS datasets will offer innovative angular capabilities for determining vegetation products over Europe and Africa thanks to concomitant multiple viewing and illumination geometries (Van-Leeuwen and Roujean, 2002). Our main concern is to retrieve fractional vegetation cover (FVC) and leaf area index (LAI) corrected from the effects of the sun-target-sensor geometry. These parameters play a critical role in the description of and land-atmosphere interactions.

The Bidirectional Reflectance Factor (BRF), which is usually reported as reflectance, is the magnitude most frequently employed in radiometry to describe the behavior of natural surfaces. Remotely sensed BRF data is the unique way for monitoring the vegetation on a global scale. Linear mixture is the basis hypothesis in some simple BRDF models (e.g. GO models or kernel-driven models) for simulation of scene reflectance or in remote sensing algorithms, e.g. spectral mixture analysis (SMA). However, the degree of validity of this assumption depends on (Qin and Gerstl, 2000): (1) the presence of multiple scattering, (2) the difficulty to determine optical properties of scene elements, (3) directional effects which can be expressed by variations of downwelling and upwelling radiative fluxes as a function of the solar and viewing directions, and (4) the scale size. For example, at a shrub scale the linear assumption is incorrect, specially in the NIR wavelengths. When the size is increased to the magnitude of kilometers, such as AVHRR and SEVIRI sensors, the linear mixture theory is approximately applicable. Furthermore, in this case the contribution of shadows is rather small (<5%), although the total fraction can be considerably higher (e.g. 18%). These results imply that at a large scale both GO and kernel-driven model are generally applicable.

SMA methods usually ignore the fact that proportions of viewed and shaded components depend on the view-sensor geometry. Only a few works have addressed these directional

effects (Asner et al., 1997; Scarth and Phinn, 2000). Another assumption of SMA is that plants are modeled as Lambertian opaque surfaces. Crown transparency is thus ignored and, therefore, information related with canopy structural parameters (LAI, leaf angle distribution (LAD), etc.) is regarded as a source of noise which may introduce a bias in the solution. On the other hand most BRDF inversion methods utilize one-dimensional models, implying thus surface homogeneity within an image pixel. Hence they are limited to address mixed landcovers pixels, which are common in coarse resolution satellites. This study aims to develop a simple, fast and operational approach to deconvolve the angular reflectance into single landcovers reflectances, attempting to solve the inconsistencies of 1-D models and linear mixture approaches. We propose an hybrid model, which combines the geometric optics of large scale canopy structure with principles of radiative transfer for volume scattering within individual crowns.

Different hybrid models have been developed in the recent years to describe the radiation regime in forest canopies (Li et al., 1995; Chen and Leblanc, 1997). These models assume a medium consisting of gaps and regions idealized by a turbid volume with a foliage density of small leaves. Gap probability is calculated based upon a geo-statistical distribution of stems. More recently, the GHOST model (Lacaze and Roujean, 2001) has been developed to address the local scale angular structure of the hot spot, which can be judged relevant for patch and regional scales.

In our model, reflectance of an individual pixel is assumed to consist of an area weighted linear combination of the soil and vegetation radiances. Canopy geometrical effects are considered in the first order scattering. The model makes a simple treatment of the multiple scattering effect using an approximate analytical solution to the radiative transfer equation. The volume scattering formulation is similar to the GHOST model. However, the between-crown gap probability is formulated in terms of the FVC and a geometric variable (η) associated with the shape of plants. A random spatial distribution of plants is assumed to simplify its computation. The invertibility of the model to retrieve FVC and LAI has been demonstrated using airborne POLDER measurements

corresponding to cropland. Model performance was also evaluated by comparing it with an accurate BRDF model of homogeneous canopies like NADIM (New Advanced Discrete Model) (Gobron et al., 1997). The next section describes the model formulation in detail. The inversion algorithm is presented in section 3. The model is validated in section 4. Finally, the conclusions and future prospects are presented in section 5.

2. MODEL FORMULATION

The reflectance of an individual pixel is assumed to consist of an area weighted linear combination of the soil and vegetation contributions:

$$R = R_v + R_s \quad (1)$$

The vegetation reflectance is expressed as a sum of single scattering (ss) and multiple scattering (ms) reflectances (Hapke, 1981; Lacaze and Roujean, 2001):

$$R_v = \frac{\omega}{4 \mu_s \mu_v} \cdot \{P(\xi) I_{ss} + [H(\mu_s) H(\mu_v) - 1] I_{ms}\} \quad (2)$$

where ω is the leaf scattering albedo, i.e. the sum of the leaf reflectance (ρ) and transmittance (τ), $\mu_{s,v} = \cos\theta_{s,v}$, ξ is the phase angle, and the factors I_{ss} and I_{ms} model the proportion of radiation flux which is single/multiple scattered by foliage elements on the downgoing and outgoing optical pathways as a whole. The Chandrasekhar function $H(\mu_{s,v})$ is used to compute multiple scattering (Hapke, 1981):

$$H(\mu_{s,v}) = \frac{1 + 2\mu_{s,v}}{1 + 2\mu_{s,v}\sqrt{1-\omega}} \quad (3)$$

$P(\xi)$ is a turbid medium phase function (Ross, 1981):

$$P(\xi) = \frac{8}{3\pi\omega} \{ \tau [(\pi - \xi) \cos\xi + \sin\xi] + \rho (\sin\xi - \xi \cos\xi) \} \quad (4)$$

The GHOST model relies on the coupling between a simple hot spot formula (Roujean, 2000) and the G-function that describes the canopy geometry. Thus single and multiple scattering processes are controlled by the mean foliage factor, G , which accounts for both the volume and the geometric components. In our model, G controls only the volume component depending on the within-crown element distribution, whereas the external geometric component depending on the crown shape and dimension is evaluated using an average theory of the gap probability.

2.1 Volume component

The proposed model assumes that the geometrical component and the volume component of the radiation fluxes can be decoupled in such a way that the flux interception of radiation can be expressed as follows:

$$I_{ss} = I_{ss,vol} \cdot I_{ss,geo} \quad I_{ms} = I_{ms,vol} \cdot I_{ms,geo} \quad (5)$$

The volume single/multiple scattered component can be described using the Beers' law:

$$I_{ss,vol} = \frac{1}{\Delta} [1 - \exp(-\Delta LAI \Omega_E \gamma / g_c)] \quad (6)$$

$$I_{ms,vol} = \frac{1}{\Delta} [1 - \exp(-\Delta' LAI \Omega_E \gamma / g_c)] \quad (7)$$

where Ω_E is the clumping index of the shoots, which quantifies the level of foliage aggregation within the tree crown. LAI is the scene leaf area index defined as half the

total needle area per unit ground surface area, g_c denotes the fractional vegetation cover and γ is a band-specific factor, which was assumed to be dependent on the leaf transmittance (e.g. Bégué, 1992). Assuming plants with similar foliar density in the scene, LAI/g_c represents an average value of the LAI of individual plants. This term is more pertinent to describe crown trees transparency than scene LAI. Δ denotes the (bidirectional) normalised extinction coefficient for singly scattered radiance. The model adopts the analytical expression derived by Roujean (2000) to the hot spot effect, i.e. coupling the downgoing and outgoing optical pathways:

$$\Delta = \sqrt{\frac{G_s^2}{\mu_s^2} + \frac{G_v^2}{\mu_v^2}} - 2 \frac{G_s G_v}{\mu_s \mu_v} \cos\xi \quad (8)$$

where G is the well-known function defined by Ross (1981) to represent the mean monodirectional projection of a unit foliage area, which depends on the LAD. For the multiple scattered component the hot spot phenomenon is usually ignored (Qin and Goel, 1995), i.e.:

$$\Delta' = \frac{G_s}{\mu_s} + \frac{G_v}{\mu_v} \quad (9)$$

2.2 Geometric component

The geometric component of the single scattering $I_{ss,geo}$ is determined by the between-crown light penetration and the visibility of illuminated objects. This component is particularly relevant for discontinuous canopies. For example, forest reflectance is dominated by the contrast between the sunlit and shaded components, especially in the visible parts of the spectrum. One question that arises is to describe the contribution of shaded and illuminated ground and crown, even when overlapping complicates the generalisation for denser canopies. Intercepted fluxes were formulated in terms of horizontal projection of the crown. Let denote by $P_0(\theta)$ the (between-crown) monodirectional gap fraction, which corresponds to the fraction of soil seen in the direction θ (Nilson, 1971). It is a biophysical variable of prime interest for remote sensing since it directly determines the single scattering process in the radiative transfer process (Weiss and Baret, 1999). LAI and fAPAR are strongly related to the monodirectional gap fraction. In fact, P_0 at particular directions provides an indirect way to estimate LAI and fAPAR (Weiss and Baret, 1999). For homogeneous Poisson distribution, the probability of observing the ground under the tree crowns in any given pixel approaches to (Jasinski and Eagleson, 1989):

$$P_0(\theta_s) = (1 - g_c)^{(\eta+1)} \quad (10)$$

where η is defined as the ratio of ground projected shadow to plant area. It absorbs all the geometric factors which relate canopy area to shadowing area into only one variable. Its analytical expression for the most common geometrical bodies is provided in Jasinski and Eagleson (1990). For example for the case of square cylinders, we have:

$$\eta = \tan\theta/b \quad (11)$$

where b is the similarity parameter, defined as the ratio of the mean width D to the mean height H . The probability of having sunlit ground P_{ig} and viewed ground P_{vg} can be expressed as follows:

$$P_{vg} = P_0(\theta_v) \quad P_{ig} = P_0(\theta_s) \quad (12)$$

A functional relationship can be also found between subpixel shaded ground P_{sg} and fractional vegetation cover:

$$P_{sg} = 1 - g_c - (1 - g_c)^{(n_s+1)} \quad (13)$$

Logically, the vertical crown cover projections in the view and sun directions are given by:

$$P_{vc} = 1 - P_0(\theta_v) \quad P_{ic} = 1 - P_0(\theta_s) \quad (14)$$

Equations (10,12-14) are applicable at large sampling scales, when imaging stands resolutions greater than the size of the tree crowns. In order to confirm these mathematical relationships, different nadir images were simulated by means of a canopy reflectance model (García-Haro and Sommer, 2002). The spatial distribution of subcanopies, dimensions, density and sun geometry were systematically altered, allowing us to evaluate the conditions in which the proposed parameterisation is applicable. For each simulated image, the subpixel proportions of shaded ground, sunlit ground, shaded crown and sunlit crown were obtained. Figure 1a shows an example corresponding to a 200m pixel with Poisson plant distribution. Figure 1b shows the relationship found between subpixel shaded ground and FVC. The figure reveals a close agreement between the values of P_{sg} derived using the simulation model (symbols) and the values obtained using Eq. 13 (dashed line). Similar simulations were undertaken varying plant distribution (regular, clumped). In general, the relationships derived from non-Poisson spatial distributions of plants differed from those predicted by Eq. (13).

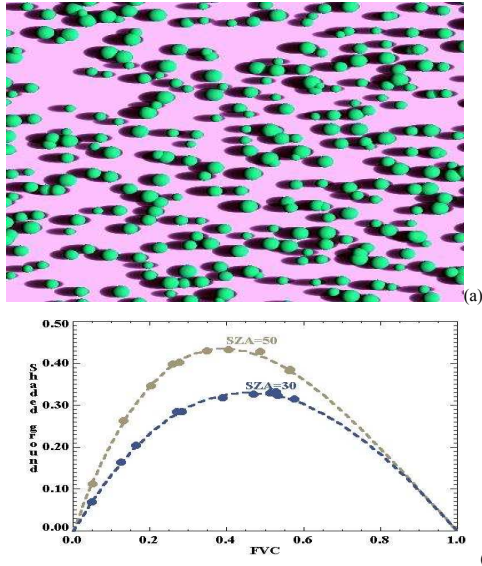


Figure 1. (a) Example of simulated nadir image. Input parameters are: $\theta_s=50^\circ$, Poisson plant distribution, FVC=0.30 and elongated plants ($b=2.5$). (b) Shaded ground P_{sg} as a function of the FVC, for two different sun zenith angles.

The probability of observing sunlit crown when P_{ic} and P_{vc} are not correlated is simply the product of both probabilities $P_{ic}P_{vc}$, where P_{ic} controls the amount of light intercepted by crowns and P_{vc} controls the contribution of visible crowns to the scene radiance. However, hot spot kernels are necessary to account for the correlation between

the two gap probabilities along sun and view directions. They should be unity when the sun and view positions align (i.e. at the hot spot) and vanish when the shift ξ of the illumination angle relative to the view angle is large enough. Direct calculations for the joint probability are, however, very complicated and require the use of certain simplifications. For example, they usually assume known the distribution of gap size inside and between tree crowns (Chen and Leblanc, 1997) or use a simple prescribed representation of crown trees sizes, shapes and distributions (Li and Strahler, 1992; Qin and Goel, 1995). The simulation of physical scenarios provides alternative methods to determine the between crown gap probability and the hot spot kernel for a wide range of biomes and spatial resolutions (García-Haro et al., 2002). GO models also allow us to address the clumping nature of vegetation at a patch scale, which is usually ignored. For example, for large pixels, the hot spot effect seems to be dominated by the radiation transmission between the gaps of macroscale elements forming the landscape such as groups of trees instead of microscale elements like needles (Lacaze et al., 2002).

We assumed that the hot spot has a minor influence on the multiple scattered interception at a crown level:

$$I_{ms,geo} = P_{ic}P_{vc} \quad (15)$$

A hot spot kernel $F_c(\xi)$ was used to modulate the dependence between the optical paths for the single scattered radiation:

$$I_{ss,geo} = P_{ic}P_{vc} + [P_{ic} - P_{ic}P_{vc}]F_c(\xi) \quad (16)$$

where $F_c(\xi)$ was obtained from the overlap function between viewing and illuminated shadows as projected on the background (Li and Strahler, 1992).

2.3 Soil component

The soil contribution R_s is expressed as the product of the background bidirectional reflectance γ_s and the vegetation transmittance T :

$$R_s = T\gamma_s \quad (17)$$

The vegetation transmittance can be expressed as the sum of the probability that a solar ray beam will reach the ground without intercepting any crown T_{geo} plus the probability of intercepting a crown without hitting any foliage element, i.e.:

$$T = T_{geo} + (1 - T_{geo})T_{vol} \quad (18)$$

The following expressions were considered for the transmissions:

$$T_{vol} = \exp(-\Delta LAI \Omega_E \gamma/g_c) \quad (19)$$

$$T_{geo} = P_{ig}P_{vg} + [P_{ig} - P_{ig}P_{vg}]F_G(\xi) \quad (20)$$

where F_G is a hot spot kernel, which tends to zero when the sun and view directions are far apart, i.e. when the viewer sees the sunlit ground through a gap different from that of illumination. In this study, it has been parameterized using a simple analytical expression. For one gap of size λ , the following hot spot function applies (Chen and Leblanc, 1997):

$$F_G(\xi) = 1 - \frac{\xi}{\tan^{-1}(\lambda/H)} \quad (21)$$

The typical size of the between-crowns gap size, λ_{ave} , was fixed, combining the dimensions of three crowns and FVC.

Model neglects side scattered diffuse radiation incident on ground surface after multiple scattering with leaves of neighboring plants. Field measurements and radiosity models all show that the side scattered light can be very significant (Roberts et al., 1990; Borel and Gerstl, 1994). The model is thus generally accurate for visible part of the solar spectrum, but less accurate at near-infrared wavelengths at which multiple scattering in plant canopies is the strongest within the solar spectrum. These non-linear effects exert a strong impact at shrub scale but they can be considered small at landscape scales when there is an horizontal mixing of vegetation types or materials (Asner et al., 1998; Qin and Gerstl, 2000).

2.4 Diffuse component

The above equations consider only the contribution of direct radiation to the reflectance. Considering also the presence of skylight irradiance, the reflectance can be expressed as a sum of the direct and isotropic diffuse components:

$$R = (1 - k_d) R_{\text{direct}} + k_d R_{\text{diffuse}} \quad (22)$$

where the component of diffuse reflectance was calculated as the average of the measurements in the principal plane. k_d denotes the fraction of diffuse irradiance, which was parameterised as follows (Lacaze and Roujean, 2001):

$$k_d = \frac{0.09}{0.09 + \mu_s} \quad (23)$$

In addition, the model allows us to derive other parameters like the entire BRDF distribution, albedo or absorptance, including the relative contribution of vegetation and soil. For example, the spectral absorptance within the canopy can be evaluated as

$$A_h = 1 - R_h - (1 - \gamma_{s,h}) T_h \quad (24)$$

where the subscript h stands for values integrated over the full view hemisphere. The fractional amount of incident photosynthetically active radiation absorbed by the vegetation canopy (fAPAR) can be evaluated by averaging the spectral canopy absorptance within the PAR region, i.e.:

$$fAPAR = \int_{400}^{700} E_{o,\lambda}(\lambda) A_h(\lambda) d\lambda \quad (25)$$

where $E_{o,\lambda}$ is the normalised solar irradiance spectrum.

3. MODEL INVERSION

The inversions are achieved simultaneously for all spectral bands, i.e. by coupling the spectral and directional data available. The variables to be retrieved are LAI and g_c . Given BRDF values r_i ($i=1, \dots, N$), representing the conditions of observation (i.e. wavelengths and view and illumination geometries), the retrievals are performed by comparing observed and modeled y_i ($i=1, \dots, N$) BRDF's. The comparisons are evaluated for a full set of prescribed canopy realisations (g_c , LAI) that cover a range of expected natural conditions. Those pairs for which the canopy model generates inputs comparable with measured data, within the limits of accuracy of data ϵ_i ($i=1, \dots, N$), i.e.:

$$(\mathbf{r} - \mathbf{y})^T \mathbf{W}^{-1} (\mathbf{r} - \mathbf{y}) \leq N \quad (26)$$

are considered as acceptable solutions, where \mathbf{W} is the covariance matrix of the measurements. The diagonal elements of \mathbf{W} are the variance ϵ^2 , which should account for both data uncertainty and unquantified errors associated with the simplifying assumptions of the theoretical model. The

distribution of solutions define a domain for g_c and LAI around the "true" values. Mean values of g_c and LAI averaged over the set of acceptable solutions are taken as solutions. This procedure not only increases the numerical stability of the inversion but also enables us to derive the uncertainty and correlation of derived parameters.

In this study, secondary model parameters (LAD, b , λ_{ave}) were fixed based on the apriori expected values. The model requires the optical properties of the underlying soil γ_s as input. It was estimated either using soil BRDFs observations in surrounding bare soil areas which were subsequently extrapolated to the POLDER observation geometries or modelled with the aid of BRDF models (Walthall et al., 1985; Jacquemod et al., 1992). In this study the extrapolation of measured BRDFs provided better results.

It was assumed for simplicity that reflectance and transmittance of leaves are similar. This assumption is accepted for many thin leaved grass and broadleaved deciduous species (Woolley, 1971). The leaf albedo ω was assessed previously by adjusting the model for each individual band. The procedure consisted in (1) setting spectral bounds that stand for the uncertainty limits of ω , and (2) adjusting them based on the best fit of the model to the directional signature, for a reduced set of canopy realisations.

Although the model has been validated against real data, a comparative analysis has also been undertaken on NADIM (Gobron et al., 1997), an invertible model of homogeneous canopies. NADIM simulates the radiation regime in the solar domain in the case of horizontally homogeneous canopies. Unlike the proposed model, which is very fast because of its analytical nature, NADIM is more expensive computationally since it explicitly solves the radiation transfer problem using a discrete representation of the canopy. The model simulates the relevant scattering processes as a function of the size (d_t) and orientation (LAD) of the leaves, as well as the total height of the canopy (H) and LAI. NADIM uses a turbid medium approach to represent the multiple scattering contribution.

NADIM has been inverted using a simple searching look-up table method, similar to the method described above. However, $g_c=1$ is implied and, therefore, the only unknown parameter is LAI. Primary model parameters (LAD, H, d_t) were fixed based on a priori expected values. Optical

parameters (ω , γ_s) were obtained using the procedure described above. Although in its original formulation NADIM assumed an isotropic soil background, soil BRDFs observations were used to represent more accurately γ_s . This allowed us to remove modelling errors found in low vegetated canopies, mainly induced by a strong soil backscattering.

4. VALIDATION

4.1 Airborne POLDER data set

The model invertibility was evaluated using data acquired by the POLDER onboard an ARAT plane during the DAISEX campaign. The experiment site selected by ESA for the DAISEX campaigns is a 3 km by 3 km area centred at 39° 3' N, 2° 5' W, which is located 28 km from Albacete (Spain), (Camacho-de Coca et al., *this issue*). Its spectral filters are centered at 443, 500, 550, 590, 670, 700, 720, 800, and 864 nm wavelength. At a typical flight altitude of 3000 m, the spatial resolution was 20 m (Leroy et al., 2001). Four flights

were undertaken during 3-5 June 1999. Each flight records around 140 spectral images, offering thus a wide range of view directions. The POLDER reflectance images were calibrated, geo-coded and corrected for atmospheric effects as it is specified in Leroy et al (2001). In this work the BRDF has been interpolated for the full range of view angles for every pixel. The BRDF was then retrieved considering uniform sites of 3x3 pixels (60x60 m²). The model has been inverted against a set of bidirectional reflectance factors taken along the principal plane, i.e. the region with the strongest anisotropy.

4.2 Results and discussion

Figures 2 and 3 show a few examples of measured BRDFs along with the values predicted by both the proposed model and NADIM, respectively. The analysis includes five bands, two sun zenith angles and four different vegetation types. The figures reveal the potential of the information contained in the directional domain of BRDF, as it was demonstrated in a preliminary work (Camacho-de Coca et al. *this issue*). Vegetation *in-situ* measurements were taken during the campaign corresponding to major agricultural units (see LAI and height values in table 1). Wheat and senescent barley presented a vertical structure. Alfalfa and legumes were lower in height, with smaller leaf size and a high LAI. Sugar beet and corn were markedly row-distributed with large contribution of the bare soil.

We can observe as both models have potential to accurately explain the spectral and angular variations of the BRDF. They capture the essential BRDF features such as bowl shape, backscattering and broad hot spot. In general, a good agreement is found between measured and modelled signatures. In general, the agreement is slightly worse when the SZA is high, i.e. when the anisotropy is higher.

The proposed model works better in the visible regions, when the first order scattering effects predominate but in the NIR region (band 8) the discrepancies are higher. In this region directional effects are less apparent due to the reduction of contrast between canopy components and the prevalence of multiple scattering. NADIM works better for dense homogeneous canopies, like alfalfa and legumes. However, it seems to be more limited when the canopy cover is lower (e.g. sugar beet), i.e. when the medium is less uniform and the reflectance is dominated by geometric effects. One source of error for both models is attributable to unquantified influences of foliage clumping. In particular, the main problems are found in erectophile canopies like wheat, with vertical structure and well-developed spikes. It causes a very pronounced 'bowl-shape' signature, especially when SZA is high. This is mainly due to the gap effect or increase of illuminated upper canopy layers viewed from the sensor at large off-nadir angles (Camacho-de Coca et al., 2002b).

Estimated parameters are presented in table 1. The inversion of both models provides reasonably accurate estimates of LAI. Furthermore, the retrievals were quite consistent, e.g. rather insensitive respect to sun zenith angle and spectral subset. In addition, the proposed model allowed us to address the FVC, obtaining values that are coherent with the field information available.

Although the inversion algorithm is satisfactory, different difficulties still arise. The main problem derives from the determination of the spectral properties, in particular for the leaf albedo. The estimation of leaf-level properties is known to be impaired by canopy-level variables like LAI. The

interdependence between leaf-level and canopy-level affects the model inversion. For example, the underestimation of leaf albedo in the visible regions usually results in an underestimation of LAI and vice versa. This may be minimised by introducing the correlation between model variables. In addition, some knowledge of ecosystem characteristics (e.g. leaf albedo measurements) can be used to constrain the solution domain, using a merit function weighted scheme (Privette et al., 1997). The merit function could be defined as a RMSE computed both on the radiometric measurements and on the canopy variables prior information (Combal et al., 2002). More research is necessary to define objectively the covariance matrix of the model parameters. Another difficulty derives from the necessity to determine the optical properties for each individual band. For further reduction of model parameters, future work will consist in coupling the model with a leaf radiative transfer model like PROSPECT (Jacquemoud et al., 1996).

Table 1. Retrieved parameters for the dominant vegetation types. Subscripts refer to: G=measured; NAD=estimated from NADIM model; M=estimated from the proposed model.

Sample	H (m)	LAI _G	LAI _{NAD}	LAI _M	FVC _M	fAPAR _M
Alfalfa	0.5-0.6	2.6	3.0	2.3	0.97	0.90
Legumes	----	----	1.2	1.2	0.80	0.86
Wheat	0.7-0.85	1.6	1.4	1.9	0.91	0.82
Sugar beet	0.1-0.15	1.2	0.6	0.9	0.55	0.64
Corn	0.1-0.2	0.3	0.2	0.2	0.27	0.26
Dry Barley	0.55-0.65	2.9	1.2	2.3	0.73	0.43

5. CONCLUSION AND PROSPECTS

This study aims to develop a simple, fast and operational approach to deconvolve the angular reflectance into single landcovers reflectances, attempting to solve the inconsistencies of 1-D models and linear mixture approaches. The result is a fast invertible canopy reflectance model of discontinuous canopies. The model relates the spectral and angular variation with the main optical and structural parameters of discontinuous canopies. A random spatial distribution of plants is assumed to simplify the gap probability computation, which may be applicable when imaging stands resolutions greater than the size of the tree crowns. Unlike BRDF models of homogeneous canopies, the model can be inverted to estimate both FVC and LAI. Moreover, the model may provide as a subproduct entire BRDF, albedo, and absorptance (including fAPAR) for the sampled scene, along with the relative contribution of vegetation and soil.

Although the model is less suited for homogeneous canopies, it can be also applicable to vegetation like grasslands and cereal crops, producing results similar to accurate BRDF models of homogeneous canopies like NADIM. The inversions revealed the model potential to combine spectral and directional information in order to increase the likely accuracy of the retrievals.

Future work will consist in coupling the model with a leaf-level radiative transfer model, which will moreover reduce the model parameters and provide a stronger connection between leaf optical properties and leaf biochemical and structural parameters. The model will be tested on existing BRDF datasets comprising different vegetation types (shrublands, forests). Intercomparisons will be also undertaken with other modelling approaches in the frame of DAISEX.

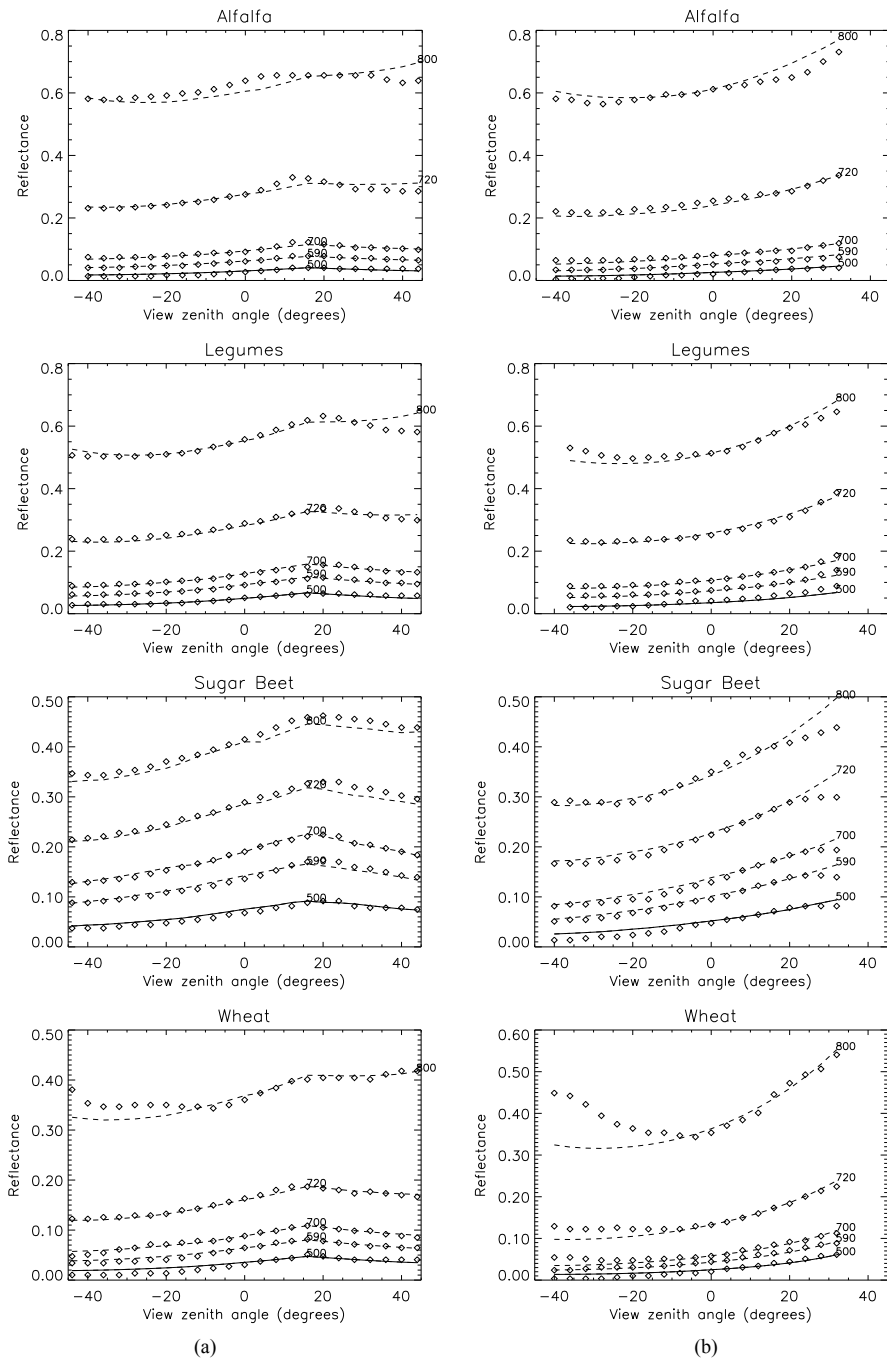


Figure 2. Comparison of directional signatures in the principal plane measured by POLDER (symbols) and simulated by the proposed model (dashed lines) at five different spectral bands (2, 4, 6, 7 and 8) over four different vegetation types. (a) Noon image ($\theta_v=17^\circ$) (b) 14:30 UT ($\theta_v=37^\circ$).

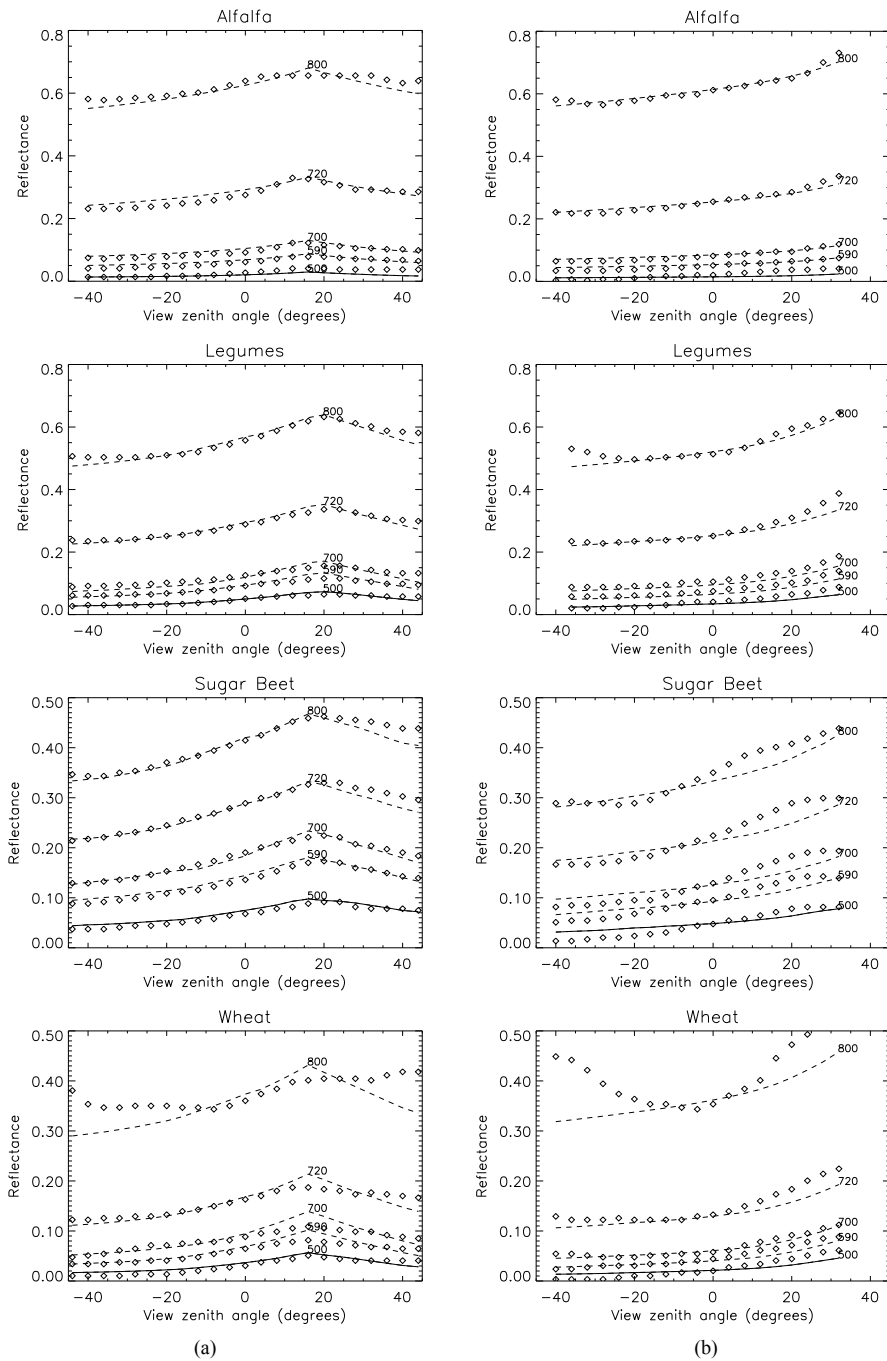


Figure 3. Comparison of directional signatures in the principal plane measured by POLDER (symbols) and simulated by NADIM (dashed lines) at five different spectral bands (2, 4, 6, 7 and 8) over four different vegetation types. (a) Noon image ($\theta_v=17^\circ$) (b) 14:30 UT ($\theta_v=37^\circ$).

ACKNOWLEDGEMENTS

This work was partially supported by the projects LSA SAF (EUMETSAT), DAISEX (ESA) and CICYT (CLI 99-0793). J. García-Haro has currently a research position (Ramon y Cajal) from MCyT, Spain. The authors want to thank N. Gobron (JRC, Ispra, Italy) for providing the NADIM model.

REFERENCES

- Asner, G.P., Wessman, C.A. and Privette, L., 1997, Unmixing the directional reflectances of AVHRR sub-pixel landcovers. *IEEE Trans. Geosci. Remote Sens.* 35: 868-878.
- Asner, G. P., Bateson, C. A., Privette, J. L., El Saleous, N., and Wessman, C. A., 1998, Estimating vegetation structural effects on carbon uptake using satellite data fusion and inverse modeling. *J. Geophys. Res.* 103:28,839-28,853.
- Bégué, A., 1993, Leaf area index, intercepted photosynthetically active radiation, and spectral vegetation indices: a sensitivity analysis for regular-clumped canopies, *Remote Sens. Environ.*, 45, 45-59.
- Borel, C. C., and Gerstl, S. A. W. 1994. Nonlinear spectral mixing models for vegetative and soil surfaces, *Remote Sens. Environ.* 47:403-416.
- Camacho-de Coca, F., García-Haro, F.J. and Meliá, J., 2002a, Quantitative analysis of cropland's BRDF anisotropy using airborne POLDER data, *Proc. 1st Int. symposium on Recent advances in quantitative remote sensing*, Torrent, in press.
- Camacho-de Coca, F., F.J. García-Haro, M.A. Gilabert and J. Meliá, 2002b, La anisotropía de la BRDF: Una nueva signatura de las cubiertas vegetales, *Revista de Teledetección*, in press.
- Combal, B., Baret, F., Weiss, M., Trubuil, A., Macé, A., Pragnère, A., Myneni, R., Knyazihin, Y. And Wang, L., 2002, Retrieval of biophysical variables from bidirectional reflectance using prior information to solve ill-posed inversion problems. *Remote Sens. Environ.*, in press.
- Chen, J.M. and Leblanc, S.G., 1997, A four-scale bidirectional reflectance model based on canopy architecture. *IEEE Trans. Geosci. Remote Sens.* 35:1316-1337.
- García-Haro, F. J and Sommer, S., 2002, A canopy reflectance model to simulate realistic remote sensing scenarios. *Remote Sens. Environ.* 81: 205-227.
- García-Haro, F.J., Camacho-de Coca, F. and Gilabert, M.A., 2002, Simulation of BRDF data to support biophysical parameters retrieval in the LSA SAF context, *Proceedings of the LSA SAF Training Workshop*, (Ed. EUMETSAT: Darmstadt), Lisbon, 8-10 July, in press.
- Gobron, N., B. Pinty, M. M. Verstraete, and Y. Govaerts, 1997, A semidiscrete model for the scattering of light by vegetation. *J. Geophys. Res.* 102(D8): 9431-9446.
- Hapke, B., 1981, Bidirectional reflectance spectroscopy: 1. Theory. *J. Geophys. Res.* 86: 3039-3054.
- Jacquemoud, S., Baret, F. and Hanocq, J.F., 1992, Modeling spectral and bi-directional soil reflectance. *Remote Sens. Environ.*, 41:123-132.
- Jacquemoud S., Ustin S.L., Verdebout J., Schmuck G., Andreoli G., Hosgood B., 1996, Estimating leaf biochemistry using the PROSPECT leaf optical properties model, *Remote Sens. Environ.*, 56:194-202
- Jasinski, M.F. and Eagleson, P.S., 1989, The structure of red-infrared scattergrams of semivegetated landscapes. *IEEE Trans. Geosci. Remote Sens.* 27: 441-451.
- Jasinski, M.F. and Eagleson, P.S., 1990, Estimation of subpixel vegetation cover using red-infrared scattergrams. *IEEE Trans. Geosci. Remote Sens.* 28: 253-267.
- Lacaze, R. and Roujean, J.L., 2001, G-function and Hot SpOT (GHOST) reflectance model. Application to multi-scale airborne POLDER measurements. *Remote Sens. Environ.*, 76:67-80.
- Lacaze, R., Chen, J.M., Roujean, J.L. and Leblanc, S.G., 2002, Retrieval of clumping index using the hot spot signatures measured by POLDER instrument. *Remote Sens. Environ.*, 79:84-95.
- Leroy, M, O. Hatecoeur, F. Ponchaut, L. Alonso-Chorda, and J. Moreno, 2001, The airborne POLDER data in the DAISEX'99 campaign, ESA SP-499, ESA Publication Division, ESTEC, The Netherlands, July 2001, 13-22.
- Li, X. and Strahler, R.A., 1992, Geometrical-optical modeling of the discrete-crown vegetation canopy: effect of crown shape and mutual shadowing. *IEEE Trans. Geosci. Remote Sens. GE-30:* 276-292.
- Nilson, T. 1971, A theoretical analysis of the frequency of gaps in plant stands. *Agric. Meteorol.* 8:25-38.
- Privette, J.L., Emery, W.J., and Schimel, D.S., 1996, Inversion of a vegetation reflectance model with NOAA AVHRR data, *Remote Sens. Environ.*, 58: 187-200.
- Qin, W. and N.S. Goel, 1995, An evaluation hotspot models for vegetation canopies, *Remote Sensing Reviews*, 13:121-159.
- Qin, W. and Gerstl, S.A.W., 2000, 3-D scene modeling of semidesert vegetation cover and its radiation regime, *Remote Sens. Environ.*, 71: 197-206.
- Roujean, J.L., M. Leroy, P.Y. Deschamps and A. Podaire, 1992, Evidence of surface reflectance bidirectional effects from a NOAA/AVHRR multitemporal data set. *Int. J. Remote Sens.*, 13:685-698.
- Roujean, J.L., 2000, A parametric hot spot model for optical remote sensing application, *Remote Sens. Environ.*, 71:197-206.
- Roberts, D. A., Adams, J. B., and Smith, M. O., 1990, Transmission and Scattering of Light by Leaves: the Effect on Spectral Mixtures, *Proc. 10th Annual IGARSS*, College Park, Md, May 20-24, pp. 1381-1384.
- Ross, J.K., 1981, The radiation regime and architecture of plants stands. *Norwell, MA: Dr. W. Junk*, 391 pp.
- Scarth, P. and Phinn, S., 2000, Determining forest structural attributes using an inverted geometric-optical model in mixed eucalypt forests, Southeast Queensland, Australia. *Remote Sens. Environ.*, 71:141-157.
- Van-Leeuwen, W.J.D. and Roujean, J.L., 2002, Land surface albedo from the synergistic use of polar (EPS) and geostationary (MSG) observing systems. An assessment of physical uncertainties, *Remote Sens. Environ.*, 81: 273-289.
- Walthall, C.L., J.M. Norman, J.M. Welles, G. Campbell, and B.L. Blad, 1985, Simple equation to approximate the bidirectional reflectance from vegetative canopies and bare soil surfaces, *Applied Optics*, 24: 383-387.
- Weiss, M. and Baret, F., 1999, Evaluation of canopy biophysical variable retrieval performances from the accumulation of large swath satellite data, *Remote Sens. Environ.*, 70: 293-306.
- Woolley, J. T., 1971, Reflectance and transmittance of light by leaves, *Plant Physiol.* 47:656-662.